Quantum reflection and Liouville transformations from wells to walls

G. Dufour,[1,*] R. Guérout,[1] A. Lambrecht,[1] and S. Reynaud[1]

[1] *Laboratoire Kastler Brossel, UPMC-Sorbonne Universités, CNRS, ENS-PSL Research University, Collège de France, Campus Jussieu, F-75252 Paris, France.*

(Dated: December 5, 2014)

Liouville transformations map in a rigorous manner one Schrödinger equation into another, with a changed scattering potential. They are used here to transform quantum reflection of an atom on an attractive *well* into reflection of the atom on a repulsive *wall*. While the scattering properties are preserved, the corresponding semiclassical descriptions are completely different. A quantitative evaluation of quantum reflection probabilities is deduced from this method.

arXiv:1412.1734v1 [quant-ph] 4 Dec 2014

Quantum reflection of atoms from the van der Waals attraction to a surface has been studied theoretically since the early days of quantum mechanics [1, 2]. Though the classical motion would be increasingly accelerated towards the surface, the quantum matter waves are reflected back with a probability that approaches unity at low energies, because the potential varies more and more rapidly close to the surface. Experiments have seen quantum reflection for He and H atoms on liquid helium films [3–5] and for ultracold atoms or molecules on solid surfaces [6–12]. Meanwhile various fundamental aspects and applications have been analyzed in a number of theoretical papers [13–23].

Paradoxical phenomena appear in the study of quantum reflection from the Casimir-Polder (CP) interaction with a surface. The potential is attractive, with characteristic inverse power laws at both ends of the physical domain $z \in]0,\infty[$ delimited by the material surface located at $z = 0$: $V(z) \simeq -C_3/z^3$ at the *cliff-side*, close to the surface and $V(z) \simeq -C_4/z^4$ at the *far-end*, away from it. Strikingly, the probability of reflection increases when the energy E of the incident atom is decreased, and increases as well when the absolute magnitude of the potential is decreased. For example, the probability of quantum reflection is larger for atoms falling onto silica bulk than onto metallic or silicon bulks [24] and is even larger for nanoporous silica [25].

In the present letter, we use Liouville transformations to study quantum reflection (QR). In quantum mechanics, a Liouville transformation maps in a rigorous manner one Schrödinger equation into another, with a changed scattering potential. In a semiclassical picture however, the problem can be transformed from QR of an atom on an attractive *well* into a problem of reflection on a repulsive *wall*. Remarkably, scattering properties are invariant under the Liouville transformation and the paradoxical features of the initial QR problem become intuitive predictions of the better defined problem of reflection on the repulsive wall. We will also obtain a quantitative evaluation of QR probabilities in this way.

We consider a cold atom of mass m incident with an energy $E > 0$ on the CP potential $V(z)$ in the half-line $z \in]0,\infty[$. For plane material surfaces, the motion orthogonal to the plane (along the $z-$direction) is decoupled from the transverse motions and described by a 1D Schrödinger equation:

$$\Psi''(z) + F(z)\,\Psi(z) = 0\,,\; F(z) \equiv \frac{2m\,(E - V(z))}{\hbar^2}\;. \quad (1)$$

Throughout the letter, primes denote differentiation with respect to the argument of the function.

In the semiclassical WKB approximation, the function $F(z)$ is seen as the square of the de Broglie wave-vector $k_{\rm dB}$ associated with the classical momentum $p \equiv \hbar k_{\rm dB}$. As the CP potential is attractive and the incident energy positive, F is positive, so that a classical particle undergoes an increasing acceleration towards the surface. For a quantum particle in contrast, QR occurs when the variation of $k_{\rm dB}$ becomes significant on a length scale of the order of the de Broglie wavelength:

$$\lambda\!\!\!^{-}_{\rm dB} \equiv \frac{\lambda_{\rm dB}}{2\pi} \equiv \frac{1}{k_{\rm dB}} = \frac{1}{\sqrt{F}}\;. \quad (2)$$

The Schrödinger equation (1) can be solved in full generality by writing its solution as a linear combination of counter-propagating WKB waves with $z-$dependent coefficients and matching it to the appropriate boundary conditions at both ends of the physical domain [13]. Matter-waves can be reflected back from the cliff-side so that the complete problem depends on the details of the physics of the surface. In this letter, we focus our attention on the one-way problem where the CP potential is crossed only once and, therefore, do not discuss this surface physics problem any longer. The numerical solution of (1) leads to reflection and transmission amplitudes depending on the incident energy E or, equivalently, of the parameter $\kappa \equiv \sqrt{2mE}/\hbar$ which is also the asymptotic value of de Broglie wavevector in the far-end.

In spite of its effectiveness, the numerical solution of the QR problem leaves open questions. First, the scattering problem, where matter waves are reflected or transmitted on the CP potential, is not well defined with the potential diverging at the cliff-side. Second, an intuitive understanding of the dependence of QR probability on the parameters is missing. The Liouville transformations considered in the following will give clear answers to these questions.

The Schrödinger equation (1) is an example of a Sturm-Liouville equation in canonical form [26], which can be submitted to transformations introduced by Liouville [27] and often named after him (see the historical notes at the end of ch.6 in [28]). We stress at this point that we use these transformations to relate exactly equivalent scattering problems, with no approximation (see a similar approach to the study of differential equations in [29]).

Liouville transformations are gauge transformations consisting in a change of coordinate $z \to \tilde{z}$, with $\tilde{z}(z)$ a smooth monotonously increasing function, and an associated rescaling of the wave-function:

$$\tilde{\Psi}(\tilde{z}) = \sqrt{\tilde{z}'(z)}\,\Psi(z) \ . \tag{3}$$

Equation (1) for Ψ is transformed under (3) into an equivalent equation for $\tilde{\Psi}$ with [28]:

$$\tilde{F}(\tilde{z}) = \frac{F(z) - \frac{1}{2}\{\tilde{z}, z\}}{\tilde{z}'(z)^2} = z'(\tilde{z})^2 F(z) + \tfrac{1}{2}\{z, \tilde{z}\} \ . \tag{4}$$

The curly braces denote the Schwarzian derivative of the coordinate transformation:

$$\{\tilde{z}, z\} = \frac{\tilde{z}'''(z)}{\tilde{z}'(z)} - \frac{3}{2}\frac{\tilde{z}''(z)^2}{\tilde{z}'(z)^2} \ . \tag{5}$$

These transformations form a group, with the composition of $z \to \tilde{z}$ and $\tilde{z} \to \hat{z}$ being a transformation $z \to \hat{z}$. The compatibility of relations obeyed by (Ψ, F), $(\tilde{\Psi}, \tilde{F})$ and $(\hat{\Psi}, \hat{F})$ is ensured by Cayley's identity:

$$\{\hat{z}, z\} = (\tilde{z}'(z))^2 \ \{\hat{z}, \tilde{z}\} + \{\tilde{z}, z\} \, . \tag{6}$$

The inverse transformation, used for the second equality in (4), is obtained by applying (6) to the case $\hat{z} = z$.

The group of transformations preserves the Wronskian of two solutions Ψ_1, Ψ_2 of the Schrödinger equation, which is a constant independent of z and skew symmetric in the exchange of the two solutions:

$$\mathcal{W}(\Psi_1, \Psi_2) = \Psi_1(z)\Psi_2'(z) - \Psi_1'(z)\Psi_2(z) \ . \tag{7}$$

In particular, when Ψ solves (1), its complex conjugate Ψ^* solves it as well. As the probability density current is proportional to the Wronskian $\mathcal{W}(\Psi^*, \Psi)$, it is invariant under the transformation. The reflection and transmission amplitudes r and t are also preserved, as they can be written in terms of Wronskians of solutions which match incoming and outgoing WKB waves [30]. They can be calculated equivalently after any Liouville transformation, with $\tilde{r} = r$ and $\tilde{t} = t$. These transformations, which do not necessarily simplify the resolution of (1), have to be considered as gauge transformations relating equivalent scattering problems to one another.

These quantum-mechanically equivalent scattering problems may correspond to extremely different classical descriptions. We now write a specific Liouville gauge which maps the initial problem of QR on an attractive well into an intuitively different problem of reflection on a repulsive wall. This choice brings clear answers to the questions discussed above, and it will allow us to uncover scaling relations between the QR probabilities and the parameters of the problem.

This specific Liouville gauge is written in terms of the WKB phase $\phi \equiv \int^z k_{\rm dB}(y)\mathrm{d}y$ associated with the classical action integral $S \equiv \hbar\phi$. We fix the freedom associated with the arbitrariness of the phase reference by enforcing $\phi(z) \to \kappa z$ at $z \to \infty$. We then choose the coordinate $\mathbf{z}$ for which we get quantities identified by boldfacing:

$$\mathbf{z} \equiv \frac{\phi}{\sqrt{\kappa\ell}} \ , \quad \mathbf{F}(\mathbf{z}) \equiv \mathbf{E} - \mathbf{V}(\mathbf{z}) \ , \tag{8}$$
$$\mathbf{E} = \kappa\ell \ , \quad \mathbf{V}(\mathbf{z}) = -\kappa\ell\sqrt{\lambda_{\rm dB}^3(z)}\left(\sqrt{\lambda_{\rm dB}(z)}\right)'' \ .$$

We have defined the length scale $\ell \equiv \sqrt{2mC_4}/\hbar$ associated with the far-end tail of the CP potential. Its introduction in (8) has been done for reasons which will become clear soon, and it leads to a dimensionless energy $\mathbf{E}$ and a dimensionless potential $\mathbf{V}$.

For the CP potential, the quantity $\mathbf{V}$ vanishes at both ends of the physical domain $z \in]0, \infty[$, that is also at both ends of the transformed domain $\mathbf{z} \in]-\infty, \infty[$, so that the problem now corresponds to a well-defined scattering problem with no interaction in the asymptotic input and output states. In striking contrast with the original QR problem, the transformed problem can have classical turning points where $\mathbf{F} = 0$ or $\mathbf{E} = \mathbf{V}$, though it corresponds to the same scattering amplitudes.

This important point is illustrated by the drawings on Fig.1, which shows the constants $\mathbf{E}$ and the functions $\mathbf{V}(\mathbf{z})$ for different scattering problems. In all cases, the original potential V is calculated for the CP interaction between an hydrogen atom and a silica bulk [24], whereas the incident energies E are respectively equal to 0.001, 0.1 and 10 neV. With $\mathbf{E}$ always positive and $\mathbf{V}(\mathbf{z})$ often positive, a logarithmic scale is used along the vertical axis, which makes some details more apparent.

The most striking feature of these plots is the appearance of classical turning points for the not too high energies considered here, so that QR on an attractive well is now intuitively understood as reflection on a wall. Other clearly visible properties are that $\mathbf{E}$ scales like $\sqrt{E}$ whereas $\mathbf{V}(\mathbf{z})$ has nearly identical peak shapes for different energies. The fact that the QR probability goes to unity when $E \to 0$ is now an immediate consequence of the increasing reflection expected for a particle with a decreasing energy $\mathbf{E}$ coming onto a wall with a peak $\mathbf{V}$.

In fact, the potentials $\mathbf{V}$ calculated for different energies tend to build up a universal function at large enough values of $\mathbf{z}$, and this universal function has a symmetrical shape. These two facts can be explained by looking at the particular model $V(z) = -C_4/z^4$, which is representative of the CP interaction in the far-end. For this simple model, $\mathbf{V}(\mathbf{z})$ is given by parametric relations (with

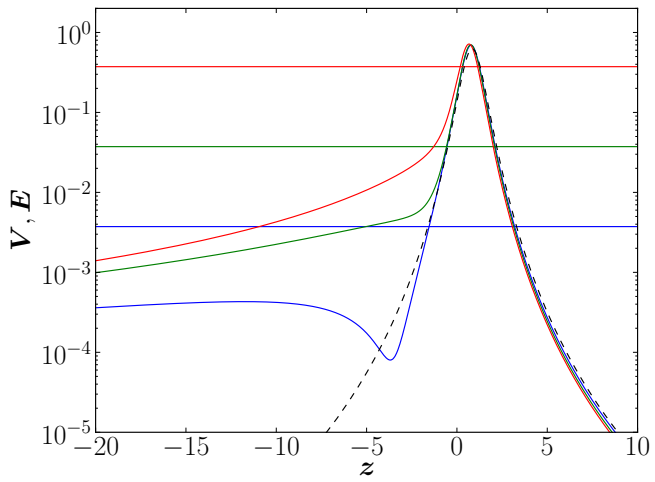

FIG. 1. [Colors online] The plots represent the constants $\mathbf{E}$ (horizontal lines) and the functions $\mathbf{V}(\mathbf{z})$ (curves) calculated for different scattering problems, corresponding to the same CP potential $V(z)$ between an hydrogen atom and a silica bulk and energies E equal to 0.001, 0.1 and 10 neV (respectively blue, green and red from the lowest to the highest value of $\mathbf{E}$, or from the lowest to the highest value of $\mathbf{V}$ in the left-hand part of the plot). The dashed (black) curve is the universal function $\mathbf{V}(\mathbf{z})$ calculated for a pure C_4 model.

$e^u \equiv z/z_0$ and $z_0 = \sqrt{\ell/\kappa}$):

$$\mathbf{V} = \frac{5}{8\cosh^3(2u)} \ , \qquad (9)$$
$$\mathbf{z} = \mathbf{z}_0 + \int_0^u \sqrt{2\cosh(2v)}\mathrm{d}v \ , \quad \mathbf{z}_0 = \frac{1}{\sqrt{\pi}}\Gamma\left(\tfrac{3}{4}\right)^2 \ .$$

This function, drawn as the dashed curve on Fig.1, reaches its peak value $\frac{5}{8}$ at $z = z_0$, which lies further and further away from the surface when the energy decreases. This also explains why the functions plotted on Fig.1 for the full CP potential tend to align on this universal form when the energy decreases. The deviations appearing on the figure correspond to values of z near the cliff-side, for which the C_4 model is indeed a poor representation as the potential behaves as $-C_3/z^3$. In the parametric definition (9), $\mathbf{V}$ is even and $\mathbf{z} - \mathbf{z}_0$ odd in the parity $u \to -u$. It follows that the universal function $\mathbf{V}(\mathbf{z})$ is symmetrical with respect to $\mathbf{z}_0$.

We come now to the discussion of the dependence of QR on the absolute magnitude of the CP potential. To do so we consider hydrogen falling onto nanoporous silica, which has a weaker CP interaction when its porosity increases [25]. Fig.2 shows the constants $\mathbf{E}$ and the functions $\mathbf{V}(\mathbf{z})$ for an energy $E = 0.01$ neV, and the potentials calculated for an hydrogen atom falling onto nanoporous silica with porosities η equal to 0%, 50% and 90%. These potentials correspond to different far-end tails, with values of C_4, and therefore ℓ, smaller and smaller when the porosity is increased. As on Fig.1, the transformed potentials $\mathbf{V}$ have nearly identical peak shapes, which tend to align on the universal curve calculated for a pure C_4 potential and shown as the dashed curve. In contrast, the transformed energies $\mathbf{E} = \kappa\ell$ are decreasing when ℓ is decreased, which immediately explains why the QR probability increases [25].

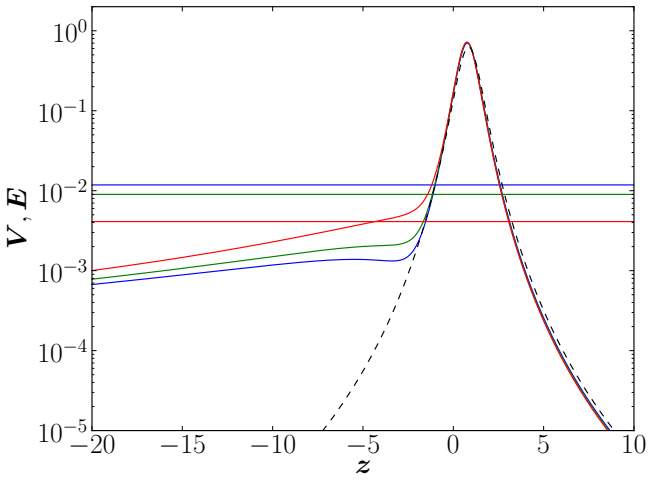

FIG. 2. [Colors online] The plots represent the constants $\mathbf{E}$ (horizontal lines) and the functions $\mathbf{V}(\mathbf{z})$ (curves) calculated for different scattering problems, corresponding to the energy $E = 0.01$ neV and the CP potentials $V(z)$ between an hydrogen atom and nanoporous silica with porosities η equal to 0%, 50% and 90% (respectively blue, green and red from the highest to the lowest value of $\mathbf{E}$, or from the lowest to the highest value of $\mathbf{V}$ in the left-hand part of the plot). The dashed (black) curve is the same as on Fig.1.

We finally discuss the values obtained for QR probabilities, by comparing the exact results for the full CP potential with those obtained for the C_4 model. To this aim, we first recall the low energy behavior of the QR probability:

$$R(\kappa) \equiv |r(\kappa)|^2 \simeq 1 - 4\kappa b \ , \quad \kappa \to 0 \ , \qquad (10)$$

where b is the opposite of the imaginary part of the scattering length [24]. For a pure C_4 model, b is known to be equal to ℓ [21], but this is not the case for the full CP potential. Table I gives ℓ and b for nanoporous silica with different porosities η ($\eta = 0\%$ for silica bulk).

η [%]	0	30	50	70	90
ℓ [a_0]	321.3	282.1	244.7	192.8	111.8
b [a_0]	272.7	227.8	187.5	134.0	57.0

TABLE I. Values of ℓ and b calculated for different porosities, measured in atomic units $a_0 \simeq 53$ pm.

We have reported on Fig.3 the calculated QR probabilities R as a function of the dimensionless parameter κb for the scattering problems discussed above. The

full blue curve represents the values calculated for silica bulks in [24], while the circles correspond to the scattering problems of Fig.2 with the same color code. The dashed black curve corresponds to the universal function $R(\kappa b)$ obtained for the pure C_4 model, with $b \equiv \ell$ in this case. A table of values of this function is available as supplemental material. The exact results on Fig.3 are hardly distinguishable from this universal function, except at large values of κb where QR probabilities are small anyway.

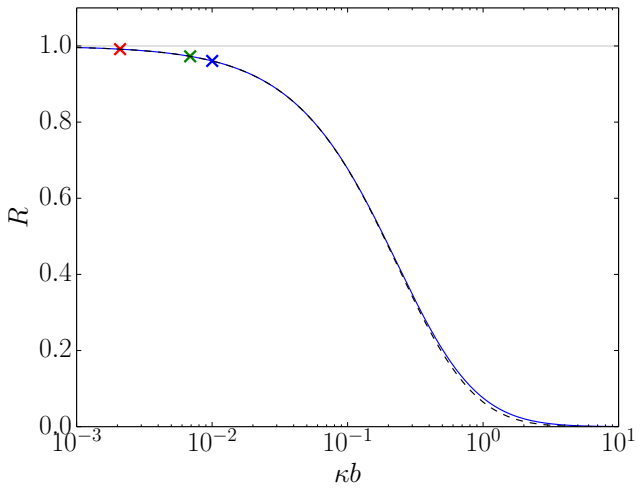

FIG. 3. [Colors online] Quantum reflection probability R shown as a function of the dimensionless parameter κb. The full blue curve represents the values calculated for silica bulks in [24], while the crosses correspond to the scattering problems of Fig.2 with the same color codes. The dashed (black) curve is the universal function R for a pure C_4 model.

In this letter, the problem of QR of an atom on a potential well has been mapped into an equivalent problem of reflection on a wall through a Liouville transformation of the Schrdinger equation. This exact transformation relates quantum scattering processes which correspond to different semiclassical pictures. It produces a new and clear interpretation of the main features of quantum reflection which were counterintuitive in the initial problem. It also allows quantitative evaluation of QR probabilities which can be obtained from the universal function corresponding to the pure C_4 model.

Acknowledgements - Thanks are due for insightful discussions to M.-T. Jaekel, V.V. Nesvizhevsky, A. Yu. Voronin, and the GBAR and GRANIT collaborations.

* gabriel.dufour@upmc.fr

[1] J. E. Lennard-Jones and A. F. Devonshire, Proc. Roy. Soc. London, **A156**, 6 (1936).
[2] J. E. Lennard-Jones and A. F. Devonshire, Proc. Roy. Soc. London, **A156**, 29 (1936).
[3] V. U. Nayak, D. O. Edwards, and N. Masuhara, Phys. Rev. Lett., **50**, 990 (1983).
[4] J. J. Berkhout, O. J. Luiten, I. D. Setija, T. W. Hijmans, T. Mizusaki, and J. T. M. Walraven, Phys. Rev. Lett., **63**, 1689 (1989).
[5] I. A. Yu, J. M. Doyle, J. C. Sandberg, C. L. Cesar, D. Kleppner, and T. J. Greytak, Phys. Rev. Lett., **71**, 1589 (1993).
[6] F. Shimizu, Phys. Rev. Lett., **86**, 987 (2001).
[7] V. Druzhinina and M. DeKieviet, Phys. Rev. Lett., **91**, 193202 (2003).
[8] T. A. Pasquini, Y. Shin, C. Sanner, M. Saba, A. Schirotzek, D. E. Pritchard, and W. Ketterle, Phys. Rev. Lett., **93**, 223201 (2004).
[9] H. Oberst, D. Kouznetsov, K. Shimizu, J.-i. Fujita, and F. Shimizu, Phys. Rev. Lett., **94**, 013203 (2005).
[10] T. A. Pasquini, M. Saba, G.-B. Jo, Y. Shin, W. Ketterle, D. E. Pritchard, T. A. Savas, and N. Mulders, Phys. Rev. Lett., **97**, 093201 (2006).
[11] B. S. Zhao, H. C. Schewe, G. Meijer, and W. Schoellkopf, Phys. Rev. Lett., **105**, 133203 (2010).
[12] B. S. Zhao, G. Meijer, and W. Schoellkopf, Science, **331**, 892 (2011).
[13] M. V. Berry and K. E. Mount, Rep. on Progr. in Phys., **35**, 315 (1972).
[14] J. Böheim, W. Brenig, and J. Stutzki, Zeitschrift für Physik B Condensed Matter, **48**, 43 (1982).
[15] D. P. Clougherty and W. Kohn, Phys. Rev. B, **46**, 4921 (1992).
[16] C. Carraro and M. W. Cole, Phys. Rev. B, **45**, 12930 (1992).
[17] C. Henkel, C. I. Westbrook, and A. Aspect, J. Opt. Soc. Am., **B13**, 233 (1996).
[18] H. Friedrich, G. Jacoby, and C. G. Meister, Phys. Rev. A, **65**, 032902 (2002).
[19] H. Friedrich and A. Jurisch, Phys. Rev. Lett., **92**, 103202 (2004).
[20] H. Friedrich and J. Trost, Physics Reports, **397**, 359 (2004).
[21] A. Y. Voronin and P. Froelich, J. Phys. B, **38**, L301 (2005).
[22] T. E. Judd, R. G. Scott, A. M. Martin, B. Kaczmarek, and T. M. Fromhold, New J. of Phys., **13**, 083020 (2011).
[23] A. Y. Voronin, V. V. Nesvizhevsky, and S. Reynaud, J. Phys. B, **45** (2012).
[24] G. Dufour, A. Gérardin, R. Guérout, A. Lambrecht, V. V. Nesvizhevsky, S. Reynaud, and A. Y. Voronin, Phys. Rev. A, **87**, 012901 (2013).
[25] G. Dufour, R. Guérout, A. Lambrecht, V. V. Nesvizhevsky, S. Reynaud, and A. Y. Voronin, Phys. Rev. A, **87**, 022506 (2013).
[26] J. Liouville, J. de math. pures et appl., **1**, 253 (1836).
[27] J. Liouville, J. de math. pures et appl., **2**, 16 (1837).
[28] F. Olver, *Asymptotics and Special Functions* (Taylor & Francis, 1997) ISBN 9781568810690.
[29] R. Milson, Int. J. of Theor. Phys., **37**, 1735 (1998).
[30] W. Whitton and J. Connor, Molec. Phys., **26**, 1511 (1973).